THE JOURNAL OF BIOLOGICAL CHEMISTRY VOL. 288, NO. 27, pp. 19661–19672, July 5, 2013
Published in the U.S.A.

Campylobacter jejuni Lipooligosaccharide Sialylation, Phosphorylation, and Amide/Ester Linkage Modifications Fine-tune Human Toll-like Receptor 4 Activation*

Received for publication, March 12, 2013, and in revised form, April 24, 2013 Published, JBC Papers in Press, April 29, 2012, DOI 10.1074/jbc.M113.468298

Holly N. Stephenson[‡1], Constance M. John[§], Neveda Naz[¶], Ozan Gundogdu[¶], Nick Dorrell[¶], Brendan W. Wren[¶], Gary A. Jarvis[§2], and Mona Bajaj-Elliott[‡]

From the [‡]Infectious Diseases and Microbiology Unit, Institute of Child Health, University College London, 30 Guilford Street, London WC1N 1EH, United Kingdom, [§]Department of Laboratory Medicine, Veterans Affairs Medical Center and University of California, San Francisco, California 94121, and [¶]Department of Pathogen Molecular Biology, London School of Hygiene and Tropical Medicine, Keppel Street, London WC1E 7HT, United Kingdom

Background: *Campylobacter jejuni* lipooligosaccharide (LOS) is a critical determinant of host innate immunity.
Results: Three structural features of the LOS moiety vary significantly between strains and in combination impact monocyte activation.
Conclusion: Variation of LOS structure suggests that LOS-TLR4 engagement during *C. jejuni* infection is strain-specific.
Significance: Source and variation of LOS structure among *C. jejuni* strains may impact host proinflammatory responses.

Campylobacter jejuni* is a leading cause of acute gastroenteritis. *C. jejuni* lipooligosaccharide (LOS) is a potent activator of Toll-like receptor (TLR) 4-mediated innate immunity. Structural variations of the LOS have been previously reported in the oligosaccharide (OS) moiety, the disaccharide lipid A (LA) backbone, and the phosphorylation of the LA. Here, we studied LOS structural variation between *C. jejuni* strains associated with different ecological sources and analyzed their ability to activate TLR4 function. MALDI-TOF MS was performed to characterize structural variation in both the OS and LA among 15 different *C. jejuni* isolates. Cytokine induction in THP-1 cells and primary monocytes was correlated with LOS structural variation in each strain. Additionally, structural variation was correlated with the source of each strain. OS sialylation, increasing abundance of LA D-glucosamine *versus* 2,3-diamino-2,3-dideoxy-D-glucose, and phosphorylation status all correlated with TLR4 activation as measured in THP-1 cells and monocytes. Importantly, LOS-induced inflammatory responses were similar to those elicited by live bacteria, highlighting the prominent contribution of the LOS component in driving host immunity. OS sialylation status but not LA structure showed significant association with strains clustering with livestock sources. Our study highlights how variations in three structural components of *C. jejuni* LOS alter TLR4 activation and consequent monocyte activation.

Campylobacter jejuni is a leading cause of acute gastroenteritis in both the industrialized and developing world. Contaminated poultry is considered to be the predominant source of infection, although transmission via non-livestock sources such as water and milk are increasingly implicated (1–3). The clinical spectrum of *C. jejuni* infection can range from asymptomatic carriage to acute inflammatory diarrhea to autoimmune complications. The presence of leukocytes in stools during the first few days of infection is indicative of an early innate inflammatory response that aids bacterial clearance while contributing to clinical disease in the susceptible (4).

Previous studies have highlighted the potential role of Toll-like receptors (TLRs)[3] in mediating early host immunity to *C. jejuni* (5, 6). The bacterium evades recognition by human TLR5 due to amino acid sequence alterations within the flagellin protein; this phenomenon has also been noted in other ϵ-proteobacteria such as *Helicobacter pylori*, suggesting that negation of TLR5-mediated antimicrobial immunity may provide strategic advantage to certain enteropathogens (7). The glycolipid lipooligosaccharide/lipopolysaccharide (LOS/LPS) moieties of *C. jejuni* and *H. pylori*, respectively, show divergent responses upon TLR4 activation. The tetraacylated *H. pylori* LPS exhibits low reactivity; in comparison, the hexaacylated *C. jejuni* LOS is a potent TLR4 agonist (5, 6, 8–10). The latter observation raises the hypothesis that *C. jejuni* LOS/TLR4 activation may contribute to the acute mucosal inflammation often seen in human infections. The association of *C. jejuni* strains with LOS modifications that promote proinflammatory responses with increased severity of enteritis supports this hypothesis (9, 11).

The structure of both the lipid A (LA) and the oligosaccharide (OS) components of the LOS/LPS moiety can significantly

* This work was supported in part by a Charlotte and Yule Bogue research fellowship from University College London (to H. N. S.), the Biomedical Research Council, UK, and Research Service of the United States Department of Veterans Affairs Merit Review Award BX000727 (to G. A. J.).

[1] Present address: Dept. of Cellular Microbiology, Max Planck Inst. for Infection Biology, Charité Platz, Berlin 10117, Germany.
[2] To whom correspondence should be addressed: Dept. 111W1, Veterans Affairs Medical Center, 4150 Clement St., San Francisco, CA 94121. E-mail: Gary.Jarvis@ucsf.edu.

[3] The abbreviations used are: TLR, Toll-like receptor; LOS, lipooligosaccharide; OS, oligosaccharide; LA, lipid A; SA, sialic acid; GBS, Guillain-Barré syndrome; GlcN, 2-amino-2-deoxy-D-glucose; GlcN3N, 2,3-diamino-2,3-dideoxy-D-glucose; PEA, phosphoethanolamine; DPLA, diphosphorylated LA; Kdo, 3-deoxy-D-manno-oct-2-ulosonic acid; Hep, heptose; Hex, hexose; HexNAc, *N*-acetylhexosamine; OAc, *O*-acetate; PPEA, phosphoryl-PEA; Neu5Ac, *N*-acetylneuraminic acid; TRIF, Toll/IL-1 receptor (TIR) domain-containing adaptor inducing IFN-β.

alter TLR4 activation and subsequent responses (12). The heterogeneous nature of *C. jejuni* LOS LA and OS structures has been noted previously (13–16). To date, 19 different genetic loci for the OS genes have been identified in *C. jejuni* strains (16). Five of these LOS classes encode sialic acid (SA) biosynthesis genes that include *neuB1* (SA synthase), *cstII* (SA transferase), and *neuA1* (CMP-Neu5Ac synthase). OS sialylation is associated with the neuropathy Guillain-Barré syndrome (GBS) and with increased TLR4 function and severity of gastroenteritis (9, 11, 17). *C. jejuni* LA is predominately hexaacylated with four primary and two secondary acyl chains (13). The LA of the majority of Gram-negative bacteria constitutes a 2-amino-2-deoxy-D-glucose (GlcN) disaccharide structure; in contrast, *C. jejuni* LA can be heterogeneous, containing 1 or 2 GlcN or 2,3-diamino-2,3-dideoxy-D-glucose (GlcN3N) residues, which leads to variation in the number (two (GlcN-GlcN) to four (GlcN3N-GlcN3N)) of amide linkages to the acyl chains. Amide linkages in *C. jejuni* LOS can influence TLR4 signaling and antimicrobial resistance (18). Additionally, *C. jejuni* LA may contain phosphate and/or phosphoethanolamine (PEA) groups, although diphosphorylated LA (DPLA) is the predominant species (19). A recent report highlighted the importance of modification of the LA backbone with PEA residues in both the activation of human TLR4 and the colonization of chickens (20).

Whole genome phylogenetic analysis divides *C. jejuni* into "livestock"- and "non-livestock"-associated clusters, the latter including water and wildlife strains (21, 22). Although *C. jejuni* strains from both clusters can be a source of human infection, any potential structural/functional variation in the LOS moiety of different strains currently remains undefined. Here, we hypothesized that livestock and non-livestock *C. jejuni* strains promote differential TLR4 activation. To test this, LOSs from 13 human *C. jejuni* isolates (and two livestock isolates) clustering within different ecological niches were studied. Among the strains tested, variation in OS sialylation, LA phosphorylation, and amide linkages was noted; importantly, all three modifications affected TLR4 activation. Genetic analysis of a cohort of 33 strains highlighted a greater propensity for OS sialylation in livestock-associated strains. Our study highlights how natural interstrain variation in *C. jejuni* LOS sialylation, amide linkage, and phosphorylation can modulate innate immunity; this variation may partly explain the clinical spectrum of gastroenteritis noted in response to this enteropathogen.

MATERIALS AND METHODS

Bacterial Strains and LOS Extraction—Fifteen *C. jejuni* strains from a previous study of 111 strains were selected for LOS isolation (see Table 2) (21). *C. jejuni* strains were grown for 24 h on 7% (v/v) blood agar plates for co-culture studies or in *Brucella* broth for LOS extraction under microaerobic conditions at 37 °C as described previously (23). Genomic DNA was isolated by phenol/chloroform extraction. Hot phenol extraction was used for LOS isolation. Briefly, freeze-dried bacterial pellets were resuspended in water and mixed 1:1 with 90% phenol. Bacterial/phenol mixtures were stirred at ~70 °C for 2 h. Mixtures were dialyzed in 1-kDa-molecular mass-cutoff tubing (Spectrum Laboratories, Rancho Dominguez, CA) to remove phenol and lyophilized prior to resuspension in 30 ml of 1 mM Tris, EDTA containing 60 μg/ml DNase (Sigma) and 30 μg/ml RNase (Sigma). The mixture was incubated at 37 °C with shaking for 4 h. Next, 30 μg/ml proteinase K (Sigma) was added, and the mixture was incubated overnight at 37 °C with gentle shaking prior to overnight dialysis. The lyophilized pellet was resuspended in deionized water and spun at 35,000 rpm at 4 °C for 4 h following resuspension in deionized water and lyophilization. LOS was quantified using a microbalance, and its purity was confirmed by SDS-PAGE and silver staining. LOS was treated with 0.05 unit/ml neuraminidase (*Arthrobacter ureafaciens* (Sigma-Aldrich)) at 37 °C overnight to remove sialic acid residues.

MALDI-TOF Mass Spectrometry—LA and *O*-deacylated and intact LOS were prepared as described previously (24, 25). MS was performed in the linear mode on a Voyager-DE STR MALDI-TOF instrument equipped with a 337-nm nitrogen laser and delayed extraction. Spectra were obtained in the negative ion mode with an average of 500 pulses per spectrum. The acceleration voltage was −20 kV. The instrument was calibrated by using the mass for the monoisotopic $(M - H)^-$ ions for bovine insulin at m/z 5728.5931, insulin B-chain at m/z 3492.6357, renin substrate at m/z 1756.9175, angiotensin II at m/z 1044.5267, and the GlcN3N-GlcN3N diphosphoryl-LA at m/z 1903.3689. During some acquisitions, *Neisseria meningitidis* strain 89I or *Neisseria gonorrhoeae* strain 1291 LOSs were utilized for internal calibration (24, 25). Spectra were analyzed using Data Explorer software with digital smoothing (Applied Biosystems, Carlsbad, CA). For high mass resolution of some intact LOSs, negative ion MALDI MS was performed on a Synapt G2 high definition MS system (Waters, Manchester, UK) with an orthogonal TOF mass analyzer in "sensitivity mode." The neodymium-doped yttrium aluminum garnet laser was operated with 355 nm at 100–200 Hz. Spectra were digitally smoothed and base line-corrected using MassLynx software.

SA Biosynthesis Pathway—SA biosynthesis genes were detected by PCR. Primers for *neuB1* gene were: forward, 5′-GCAGGnGCTAAGATnATAAAnCAnCAAAC-3′; reverse, 5′-TAATnCTnACTACnCTnGCAAAnGCAAAATCAAT-3′. Primers for *orf7ab*, *orf7c*, *orf8ab*, *orf8c*, and *htrB* genes have been described (15).

TNFα Expression by THP-1 and Primary Human Monocytes—Monocytic THP-1 cells were differentiated with 10 ng/ml phorbol 12-myristate 13-acetate in RPMI 1640 medium with 10% fetal calf serum (FCS) overnight. A 96-well plate was seeded with THP-1 cells (1×10^5 cells/well), which were allowed to adhere for 2 h prior to stimulation with either *C. jejuni* at a multiplicity of infection of 10 or with the corresponding LOS. For some experiments, cells were treated with lipid IVa (Avanti Polar Lipids, Alabaster, AL) for 1 h prior to LOS treatment. $CD14^+$ monocytes were isolated from the peripheral mononuclear cell fraction of blood from healthy adult volunteers using $CD14^+$ bead selection according to the manufacturer's protocol (Miltenyi Biotec, Surrey, UK). The monocytes were seeded in 96-well plates (1×10^5/well) and stimulated with LOS. TNFα levels were measured by ELISA 20 h poststimulation (eBioscience, San Diego, CA).

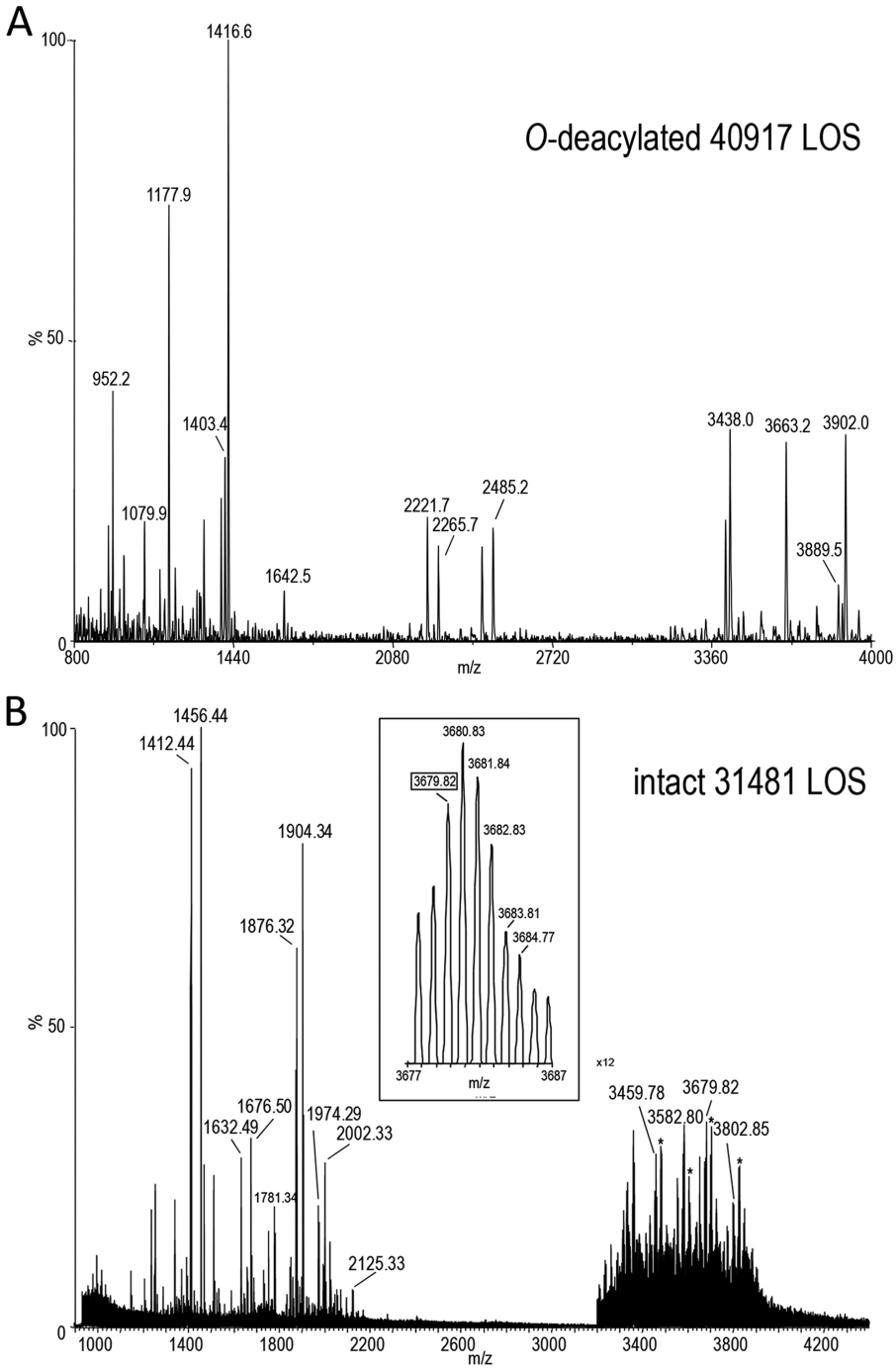

FIGURE 1. **Negative ion MALDI-TOF spectra for *O*-deacylated and intact *C. jejuni* LOS.** Representative MALDI-TOF MS spectra for *O*-deacylated LOS of strain 40917 (*A*) and intact LOS of strain 31481 (*B*). Observed peaks are postulated to be due to Y-type reducing terminal lipid A fragment ions, non-reducing terminal B-type OS fragment ions, and ions for the entire intact or *O*-deacylated LOS. In the *inset* in the high resolution spectrum (*B*), the labeled masses represent the monoisotopic ions. The *asterisks* in *B* indicate peaks for sodiated $(M + Na - 2H)^-$ ions.

Statistical Analysis—Statistical analysis was performed using Prism 5 software (GraphPad, La Jolla, CA). For comparison of more than two groups in the same experiment, repeated measures analysis of variance was applied to parametric data using the Tukey post-test to compare columns of data.

RESULTS

C. jejuni LOS Structure—To investigate the LOS/TLR4 structure-function relationship of livestock *versus* non-livestock *C. jejuni*, the LOSs from 15 strains (seven from the livestock cluster (including reference strain 11168H) and eight from the non-livestock cluster (21)) were purified. Negative ion MALDI-TOF MS was performed on both the intact and the *O*-deacylated LOS species. MALDI-TOF MS was also performed on the LA isolated from the LOSs of 10 strains. Of the seven livestock-associated strains, three were human clinical isolates from diarrheal (±blood) patients, two were from asymptomatic carriers, and two were from colonized livestock. Of the eight non-live-

TABLE 1

Molecular and fragment ion peaks in spectrum of O-deacylated 40917 (A) and intact 31481 LOS (B)

A

Observed (M-H)$^-$	Proposed Composition	Calculated (M-H)$^-$	Difference (Da)
3902.0	DPLA[a] with C16:0 [under *O*-deacylated] 2Kdo 2Hep P 6Hex 3HexNAc	3902.9	- 0.9
3889.5	DPLA with C14:0(3-OH) [under *O*-deacylated] 2Kdo 2Hep P 6Hex 3HexNAc	3890.9	-1.4
3683.2	DPLA with C16:0 [under *O*-deacylated] Kdo 2Hep P 6Hex 3HexNAc	3682.7	+0.5
3438.0	HexN-HexN DPLA [less C14:0(3-OH)] 2Kdo 2Hep P 6Hex 3HexNAc	3439.1	-1.1
2485.2[b]	2Kdo 2Hep P 6Hex 3HexNAc	2486.1	-0.9
2265.7	Kdo 2Hep P 6Hex 3HexNAc	2265.9	-0.2
2221.7[c]	Kdo 2Hep P 6Hex 3HexNAc - (CO_2)	2221.9	-0.2
1642.5[d]	DPLA with C16:0 C14:0(3-OH) [under *O*-deacylated]	1642.1	+0.4
1416.6	DPLA with C16:0 [under *O*-deacylated]	1415.8	+0.8
1403.4	DPLA with C14:0(3-OH) [under *O*-deacylated]	1403.7	-0.3
1177.9	DPLA	1177.4	+0.5
1079.9[e]	DPLA - (H_3PO_4)	1079.4	+0.5
952.2	HexN HexN DPLA [less C14:0(3-OH)]	952.0	+0.2

B

Observed (M-H)$^-$	Proposed Composition	Calculated (M-H)$^-$	Difference (PPM)
3802.85	DPLA[f] 2Kdo 2Hep 3PEA 2Hex 2HexNAc	3802.86	-2.6
3679.82	DPLA 2Kdo 2Hep 2PEA 2Hex 2HexNAc	3679.85	-8.1
3582.80	DPLA Kdo 2Hep 3PEA 2Hex 2HexNAc	3582.80	0.0
3459.78	DPLA Kdo 2Hep 2PEA 2Hex 2HexNAc	3459.79	-2.9
2125.33[d]	DPLA 2PEA	2125.34	-4.7
2002.33	DPLA PEA	2002.33	0.0
1974.29	DPLA PEA with a C14:0 replacing C16:0	1974.30	-5.1
1904.34[e]	DPLA PEA - (H_3PO_4)	1904.35	-5.3
1876.32	DPLA PEA with C14:0 replacing C16:0 - (H_3PO_4)	1876.32	0.0
1781.34	DPLA - (H_3PO_4)	1781.34	0.0
1676.50[b]	2Kdo 2Hep PEA 2Hex, 2HexNAc	1676.51	-6.0
1632.49[c]	2Kdo 2Hep PEA 2Hex 2HexNAc - (CO_2)	1632.52	-18.4
1456.44	Kdo 2Hep PEA 2Hex 2HexNAc	1456.45	-6.9
1412.44	Kdo 2Hep PEA 2Hex 2HexNAc - (CO_2)	1412.46	-14.2

[a] DPLA represents 2-amino-2-deoxy-D-hexose and 2,3-diamino-2,3-dideoxy-D-hexose (HexN-HexN3N) with two phosphate (P) and three hydroxymyristic acid (C14:0(3-OH)) moieties after *O*-deacylation.
[b] Italics represent non-reducing terminal B-type OS fragment ions from prompt fragmentation.
[c] Non-reducing terminal B-type OS fragment ions from prompt fragmentation with loss of CO_2.
[d] Bold represents reducing terminal Y-type LA fragment ions from prompt fragmentation.
[e] Prompt fragmentation producing LA ions with loss of H_3PO_4.
[f] DPLA represents HexN-HexN3N with two phosphate (P), four hydroxymyristic acid (C14:0(3-OH)), and two palmitic acid (C16:0) moieties.

stock-associated strains, four were human clinical isolates from diarrheal (±blood) patients, and four were from asymptomatic carriers.

Representative spectra of low and high resolution MS spectra of *O*-deacylated and intact LOS from two of the 15 strains are shown in Fig. 1, *A* and *B*, respectively, with proposed compositions for the major molecular and fragment ions presented in Table 1, A and B, respectively. The majority of OS compositions proposed for the 15 strains are based on the non-reducing terminal B-type fragment ions of *O*-deacylated LOS (Table 2) (26) and the components of the *C. jejuni* OS reported previously (19, 27). For strains 32787 and 43205 with unusual OS structure, data were obtained from high resolution negative ion MALDI performed on the Synapt G2 high definition MS system with an orthogonal TOF mass analyzer (Table 2B). As shown in the *inset* spectrum of the intact LOS from strain 31481 (Fig. 1*B*), base-line separation of monoisotopic peaks for the intact molecular $(M - H)^-$ ions was obtained. In general, OS fragment ion peaks in the negative ion MALDI spectra of the intact or *O*-deacylated LOS could be distinguished by the presence of lower mass peaks for the characteristic additional losses of CO_2 (44 Da) from 3-deoxy-D-manno-oct-2-ulosonic acid (Kdo) and loss of the labile Kdo moiety (220 Da) (Fig. 1, *A* and *B*, and Table 1, A and B).

Compositions proposed for monoisotopic peaks for the highest mass OS fragment ions that were detected for intact LOS from strains 32787 and 43205 are presented in Table 2B. The monoisotopic masses of these prompt B-type oligosaccharide ions were analyzed with a computer algorithm to determine potential compositions (28). The monosaccharides and other components used in the algorithm included PEA, phosphate, Gly, and *O*-acetate, which have been reported previously in the LOS of *C. jejuni* (19, 27). For strain 32787, the peak observed at *m*/*z* 2282.7402 was consistent with a composition of 2 Kdo, 2 heptose (Hep), and 7 hexose (Hex) residues; *N*-acetylhexosamine (HexNAc); phosphate; and *O*-acetate (OAc) (Table 2B). However, the data obtained did not allow distinction between this and a composition with a PPEA moiety (202.9747 Da) rather than a HexNAc (203.0794), which would differ from that observed by 80.4 ppm. One other potential composition is 2 Kdo, 2 Hep, 4 Hex, 3 HexNAc, OAc, and 2 phosphate residues for which the calculated mass differed from that observed by 49.1 ppm. Using previously identified components, only a single composition was found to be consistent with the monoisotopic exact mass for the OS fragment ions detected at *m*/*z* 2402.7959 in the spectrum of the intact LOS from strain 43205 (Table 2B). The absence of peaks corresponding to loss of SA (−291) and the absence of SA biosynthesis genes indicated that strain 56519 did not contain an SA moiety on its OS (Table 2A).

Collectively, the data are in accord with the conserved presence of 2 Kdo and 2 Hep residues and a PEA or phosphate residue on the inner core of all strains except 64555, which apparently lacks a phosphoryl moiety (Table 2A) (19). The OS contained 2–6 Hex residues, and in nine strains, SA was identified. Interestingly, the LOSs of all seven livestock strains were sialylated, but LOSs of only two of eight non-livestock strains were sialylated (Table 2; $p = 0.01$). Of the strains associated with diarrhea or asymptomatic infection, SA was detected in three of seven and four of six structures, respectively, suggesting that SA is not a determinant of asymptomatic infection (Table 2). However, LOS sialylation is known to be associated with increased severity of gastroenteritis as well as with the onset of GBS (11, 17); in this context, it was interesting to identify a greater propensity for livestock-associated strains to contain SA.

SA Biosynthesis Pathway—To further explore the association of SA with the livestock clade, a further 18 *C. jejuni* human clinical isolates in addition to the original 15 strains were investigated for the presence of the SA biosynthesis pathway by PCR. All nine SA-positive strains (by MS) were *neuB1*-positive. One

TABLE 2
Non-reducing terminal B-type OS fragment ion peaks of LOS in low resolution (A) and high resolution (B) MALDI-TOF MS

A

Strain	Clade[a]	Clinical Symptoms[b]	Proposed OS Composition[c]	Observed $(M-H)^-$	Calculated $(M-H)^-$	Difference (Da)
11168H	L	D	2Kdo PEA 2Hep 6Hex HexNAc NeuAc	2414.8	2414.1	0.7
45557	L	BD	2Kdo PEA 2Hep 6Hex HexNAc NeuAc	2414.3	2414.1	0.2
31485	L	A	2Kdo PEA 2Hep 6Hex HexNAc NeuAc	2414.6	2414.1	0.5
32799	L	A	2Kdo PEA 2Hep 4Hex HexNAc 2NeuAc	2382.5	2381.0	1.5
KJShpsm4	L	N/A	2Kdo PEA 2Hep 5Hex HexNAc NeuAc	2252.0	2251.9	0.1
KJCattle8	L	N/A	2Kdo PEA 2Hep 2Hex 2HexNAc NeuAc	1968.3	1968.7	-0.4
56282	L	D	2Kdo PEA 2Hep 4Hex HexNAc 2NeuAc	2382.8	2381.0	1.8
33106	NL	A	2Kdo PEA 2Hep 3Hex HexNAc NeuAc	1927.9	1927.6	0.3
33084	NL	A	2Kdo PEA 2Hep 3Hex 2NeuAc	2017.5	2015.7	1.8
40917	NL	BD	2Kdo P 2Hep 6Hex 3HexNAc	2485.5	2486.1	-0.6
31481	NL	A	2Kdo PEA 2Hep 2Hex 2HexNAc	1676.9	1677.4	-0.5
64555	NL	BD	2Kdo 2Hep 7Hex HexNAc	2159.7	2161.9	-1.2
56519	NL	BD	Not determined			

B

Strain	Clade[a]	Clinical Symptoms[b]	Proposed OS Composition[d]	Observed $(M-H)^-$	Calculated $(M-H)^-$	Difference (PPM)
32787	NL	A	2Kdo P 2Hep 7Hex HexNAc OAc	2282.7402	2282.6614	34.5
43205	NL	BD	2Kdo P 2Hep 8Hex HexNAc	2402.7959	2402.7036	38.4

[a] L, livestock; NL, non-livestock.
[b] D, diarrhea; BD, bloody diarrhea; A, asymptomatic; N/A, not applicable.
[c] Average masses of residues (in kilodaltons) used are as follows: Kdo, 220.2; Hep, 192.2; Hex, 162.1; HexNAc, 203.2; Neu5Ac, 291.3; PEA, 123.0; phosphate (P), 80.0; OAc, 42.0.
[d] Exact masses of residues used (in kilodaltons) are as follows: Kdo, 220.1; Hep, 192.1; Hex, 162.1; HexNAc, 203.1; Neu5Ac, 291.1; PEA, 123.0; phosphate (P), 80.0; OAc, 42.0.

TABLE 3
PCR analysis reveals association of SA synthesis genes with livestock strains

Non-livestock strain[a]	NeuB1	Class A/B	Class C	Livestock strain[a]	NeuB1	Class A/B	Class C
33106	+	+	−	11168H	+	−	+
33084	+	+	−	45557	+	−	+
40917	+	−	+	31485	+	−	+
31481	−	−	−	32799	+	+	−
56519	−	−	−	56282	+	+	−
32787	−	−	−	44811	+	−	+
64555	−	−	−	59161	+	−	+
43205	−	−	−	59214	+	+	−
44119	−	−	−	30280	+	−	+
63326	+	+	−	44958	+	+	−
62914	−	−	−	30328	+	−	+
45631	−	−	−	58473	+	+	−
59364	−	−	−	48612	+	−	+
52368	−	−	−				
56832	+	+	−				
38353	−	−	−				
12241	+	+	−				
53259	+	+	−				
35799	+	+	−				
62567	+	−	+				

[a] PCR analysis used primers that anneal to *neuB1* genes to identify strains that encode the SA biosynthesis pathway for human clinical isolates that clustered with either the non-livestock or livestock clades (21). Primers described previously (15) were used to distinguish strains from SA-positive LOS classes A/B from C.

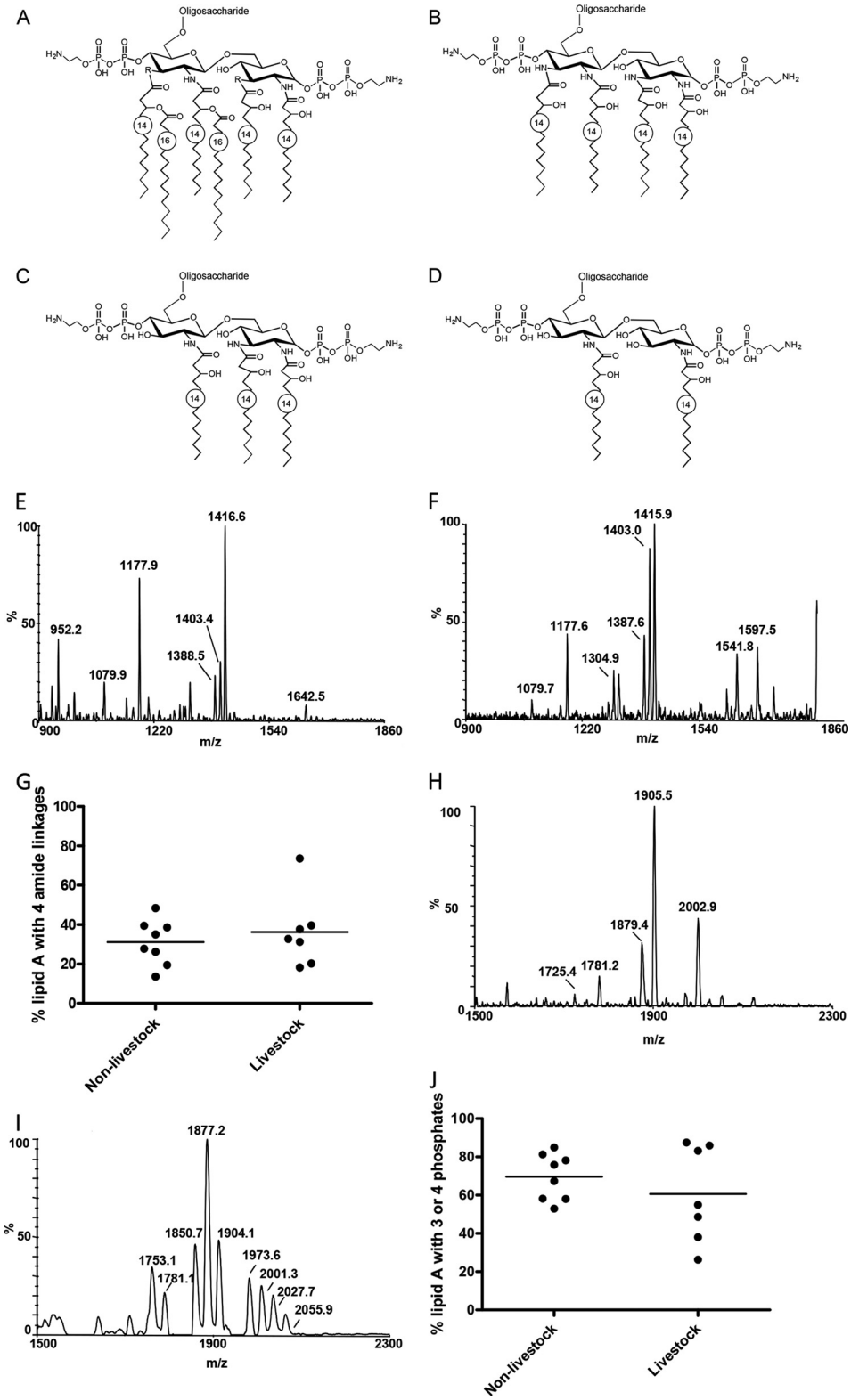

FIGURE 2. **Variation in the number of amide linkages and phosphorylation in *C. jejuni* LA.** *A*, hexaacylated *C. jejuni* lipid A with GlcN (R = O) and/or GlcN3N (R = N) disaccharide backbone originally described in Ref. 13 and confirmed in the present study. *O*-Deacylated LA composed of a GlcN3N-GlcN3N disaccharide backbone with four amide-linked acyl chains (*B*), a GlcN-GlcN3N disaccharide backbone with three amide-linked acyl chains (*C*), or a GlcN-GlcN disaccharide backbone with two amide-linked acyl chains (*D*) is shown. The LA backbone is depicted with two phosphate and two phosphoethanolamine groups, although the abundance of these modifications can vary. Y-type reducing terminal LA fragment ions were observed as shown in the portion of the negative ion MALDI-TOF MS spectra of the *O*-deacylated LOS of strain 40917 (*E*) and 31485 (*F*). *G*, the relative abundance of amide linkages was assessed by summing the areas of peaks corresponding to four amide linkages and expressing this as a percentage of the areas of all LA peaks observed in the MS analysis. Portions of negative ion MALDI-TOF spectra of the intact lipid of strains 33106 (*H*) and KJCattle8 (*I*) in which postulated Y-type LA fragment ions were observed are shown. *J*, the relative abundance of LA with three or four phosphoryl groups was calculated by summing the area of peaks corresponding to LA with three or four phosphoryl moieties and expressing this as a percentage of the total area of all LA peaks observed.

strain (40917) was found to be *neuB1*-positive but lacked SA by MS, suggesting a possible role for phase variation in this strain. All 13 human isolates clustering within the livestock cluster and only nine of 20 within the non-livestock cluster contained the *neuB1* gene (Table 3; $p = 0.003$). Taken together, the data support the hypothesis that LOS sialylation is a genetic/structural feature that may contribute to distinguishing strains from different sources. Further analysis was performed to assess LOS classification. Five of 13 livestock and seven of nine non-livestock SA-positive strains belonged to LOS class A/B (Table 3), suggesting that the specific LOS class is not a defining feature between the SA-positive strains associated with different ecological niches.

Lipid A Structure—The LA moiety is the principal ligand for TLR4 (29). We next assessed the LA acyl chain linkage and phosphorylation status of the *C. jejuni* strains. Anhydrous hydrazine hydrolyzes ester but not amide linkages, thus allowing detection of the *N*-linked acyl groups (Fig. 2, *A–D*). MS spectra for *O*-deacylated LOS reducing terminal Y-type negative ions containing the LA $(M - H)^-$ from two representative strains, 40917 and 31485, are shown (Fig. 2, *E* and *F*). The presence of a GlcN3N-GlcN3N (four amide linkages; calculated *m*/*z* 1402.8) and a GlcN3N-GlcN (three amide linkages; calculated *m*/*z* 1177.4) LA backbone containing 2 phosphate residues was observed for both strains. Ions (calculated *m*/*z* 952.0) consistent with the expression of LA with only two amide linkages, GlcN-GlcN, were apparent for 40917 LOS. Despite increased co-incubation time of LOS with hydrazine from 20 min to 2 h, complete removal of the *O*-linked fatty acid chains was not achieved (under *O*-deacylated; calculated *m*/*z* 1641.2 and *m*/*z* 1415.8 for the GlcN3N-GlcN3N and GlcN3N-GlcN species, respectively). Peaks corresponding to the loss of H_3PO_4 (98 Da) at calculated *m*/*z* 1304.8 and 1079.4 (under *O*-deacylated at calculated *m*/*z* 1543.2 and 1317.8) were also detected (Table 4).

The proportion of the GlcN3N-GlcN3N was determined by expressing the abundance of all the fragment ion peaks corresponding to GlcN3N-GlcN3N (from two spectra) relative to the abundance of all of the LA fragment ion peaks (Table 4). GlcN3N-GlcN was the predominant disaccharide. The relative abundance of LA with four amide linkages varied significantly (range, 13.7–73.7%; mean, 33.5%; standard deviation, 14.7%); however, this feature showed no correlation with the phylogenetic clusters (Fig. 2*G*). Furthermore, the clinical presentation of each strain did not correlate with the number of amide linkages (data not shown).

As *O*-deacylation of LOS also hydrolyzes some of the relatively labile phosphate and PEA residues, MALDI-TOF was performed on the native LOS to characterize the relative abundance of LA phosphorylation. Calculated masses for LA fragment ions with varying phosphorylation and GlcN-GlcN backbone composition for the native LOS are listed in Table 4B. Peaks similar to those shown were detected for GlcN3N-GlcN and GlcN3N-GlcN3N that differed from the GlcN-GlcN LA by −1 and −2 Da, respectively.

MS spectra for intact LOS reducing terminal Y-type negative ions containing the LA $(M - H)^-$ from two representative strains, 33106 and KJCattle8, are shown (Fig. 2, *H* and *I*). The most abundant peaks were consistent with the expression of a

TABLE 4
Lipid A fragment ion peaks of O-deacylated LOS (A) and GlcN-GlcN lipid A fragment ion peaks of intact LOS (B)

A

O-deacylated Lipid A Proposed Composition[a]	Calculated $(M-H)^-$
GlcN-GlcN 2P - (H_3PO_4)	854.0
GlcN-GlcN 2P[b]	924.0
GlcN-GlcN 2P	952.0
GlcN-GlcN 2P [under *O*-deacylated]	1190.4
GlcN-GlcN3N 2P - (H_3PO_4)	1079.4
GlcN-GlcN3N 2P	1149.4
GlcN-GlcN3N 2P	1177.4
GlcN-GlcN3N 2P [under *O*-deacylated]	1415.8
GlcN3N-GlcN3N 2P - (H_3PO_4)	1304.8
GlcN3N-GlcN3N 2P	1374.7
GlcN3N-GlcN3N 2P	1402.8
GlcN3N-GlcN3N 2P [under *O*-deacylated]	1641.2

B

Intact Lipid A Proposed Composition[c]	Calculated $(M-H)^-$
GlcN-GlcN P - (H_3PO_4)	1703.6
GlcN-GlcN P	1773.6
GlcN-GlcN 2P - (H_3PO_4)	1783.6
GlcN-GlcN P	1801.6
GlcN-GlcN P PEA - (H_3PO_4)	1826.6
GlcN-GlcN 2P	1853.6
GlcN-GlcN 2P	1881.6
GlcN-GlcN P PEA	1896.6
GlcN-GlcN 2P PEA - (H_3PO_4)	1906.6
GlcN-GlcN P PEA	1924.7
GlcN-GlcN 2P PEA	1976.6
GlcN-GlcN 2P PEA	2004.6
GlcN-GlcN 2P 2PEA - (H_3PO_4)	2029.7
GlcN-GlcN 2P 2PEA	2099.6
GlcN-GlcN 2P 2PEA	2127.7
GlcN-GlcN 2P 3PEA - (H_3PO_4)	2152.7
GlcN-GlcN 2P 3PEA	2222.6
GlcN-GlcN 2P 3PEA	2250.7

[a] Reducing terminal Y-type LA fragment ions of *O*-deacylated LA composed of two GlcN3N-GlcN3N (four amides), two GlcN-GlcN (two amides), or GlcN-GlcN3N (three amides) moieties. Typically, only DPLA without PEA was detected.
[b] Italics represent reducing terminal Y-type LA fragment ions that are <28 Da and have a C12:0(3-OH) replacing a C14:0(3-OH) or a C14:0 replacing a C16:0 moiety.
[c] Reducing terminal Y-type LA fragment ions of intact LA. As an example, fragment ions of LA composed of GlcN-GlcN (two amides) are presented.

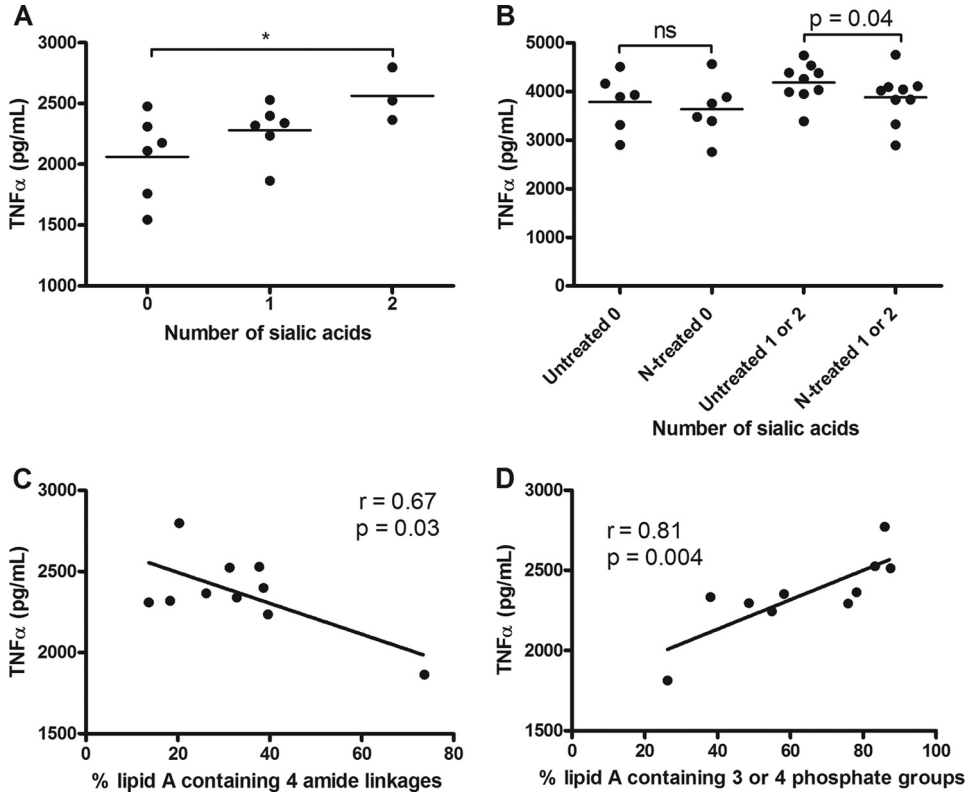

FIGURE 3. **Impact of *C. jejuni* LOS sialylation, amide linkages, and phosphorylation on TNFα induction in THP-1 cells.** THP-1 cells were stimulated with 10 ng/ml LOS for 20 h, and TNFα levels were assessed by ELISA. TNFα levels were compared with the level of sialylation of the LOS from individual strains (*A*), levels from neuraminidase-treated LOS (*N-treated; B*), the relative abundance of four amide linkages (*C*), and the relative abundances of three or four phosphoryl moieties based on the areas of the respective LA peaks for each molecule (*D*). Data points represent mean values for an individual strain from a minimum of four independent experiments. *A*, one-way analysis of variance (*, $p < 0.05$). *B*, unpaired Student's *t* test analysis (*ns*, not significant). *C* and *D*, linear regression analyses were performed.

DPLA with a single PEA moiety for strain 33106 (calculated *m*/*z* 2004.6) with an additional fragmentation causing loss of H_3PO_4 (98 Da; calculated *m*/*z* 1906.6; Fig. 2*H*). For KJCattle8, the most abundant peaks were indicative of DPLA lacking PEA (calculated *m*/*z* 1881.6 with additional loss of H_3PO_4 at *m*/*z* 1783.6 Da; Fig. 2*I*). Minor peaks in other spectra included those consistent with fragment ions for two PEA-substituted DPLA at a calculated *m*/*z* of 2127.7 with ions observed for additional loss of H_3PO_4 at *m*/*z* 2029.7 and three PEA-modified DPLA at *m*/*z* 2250.7 with ions for additional loss of H_3PO_4 at *m*/*z* 2152.7 (data not shown).

As illustrated in the intact LOS spectrum from strain KJCattle8 (Fig. 2*I*), fragment ion peaks were consistent with PEA DPLA with one hydroxylaurate acyl group instead of a hydroxymyristate (−28 Da; observed *m*/*z* 1973.6). We confirmed the presence or absence of variation in acyl chain length by analysis of the *O*-deacylated spectra when assigning LA composition to the similar ions: DPLA (calculated *m*/*z* 1881.6) and C14 PEA DPLA with loss of H_3PO_4 (calculated *m*/*z* 1878.2).

To compare the level of phosphorylation between the different strains, the abundance of tri- (2P PEA) or tetraphosphorylated (2P 2PEA) LA fragment ions was calculated relative to the fragment ions of all of the LA species for each strain (Fig. 2*J*). Although wide diversity in the level of phosphorylation was noted (percentage of tri- or tetraphosphorylated LA ranged between 26.3 and 87.5%; mean, 65.4%; standard deviation, ±19.0%), this did not correlate with the phylogenetic cluster. Furthermore, the clinical presentation of an individual strain did not correlate with the phosphorylation status (data not shown).

TNFα Expression by THP-1 Cells and Primary Human Monocytes—To assess the impact of LOS modifications on innate immunity, TNFα expression was chosen as a marker for LOS-mediated TLR4 activation. TNFα is a well characterized proinflammatory cytokine produced by monocytes in response to LOS/LPS via TLR4-MyD88-dependent signaling and serves as an accurate marker for the induction of other proinflammatory cytokines such as IL-1β, IL-6, and MIP-1β in response to TLR4 activation (24, 25, 30, 31). Phorbol 12-myristate 13-acetate-differentiated THP-1 cells were stimulated with purified LOS (10 ng/ml) for 20 h prior to cytokine analysis. Significant TNFα induction in response to all purified LOSs was observed. Importantly, a statistically significant correlation in TNFα levels and the degree of sialylation was noted (Fig. 3*A*; $p < 0.05$ between 0 and 2 residues). Treatment of LOS with neuraminidase reduced cytokine levels, confirming the potential role of SA in host TNFα expression (Fig. 3*B*; $p = 0.04$).

The presence of an ester linkage between the acyl chain and the LA backbone is known to increase TLR4 activity (18). To assess the impact of natural variability in the amide/ester links and phosphorylation status on cytokine induction, linear regression analyses were performed. The relative abundance of four amide linkages correlated with TNFα induction (Fig. 3*C*; $r = 0.67$; $p = 0.03$). Additionally, the phosphorylation status

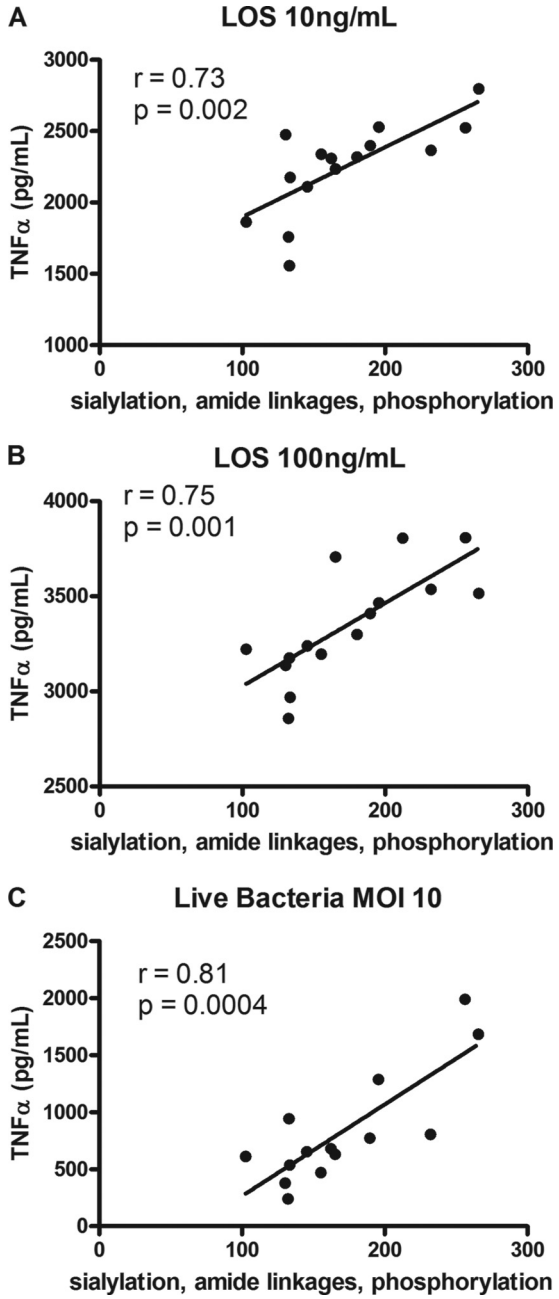

FIGURE 4. **Combinatorial effect of *C. jejuni* lipooligosaccharide sialylation, amide linkages, and phosphorylation on TNF-α induction in THP-1 cells.** Supernatants from THP-1 cells stimulated with 10 ng/ml isolated LOS (*A*), 100 ng/ml isolated LOS (*B*), or live bacteria at a multiplicity of infection (*MOI*) 10 for 20 h (*C*) were assessed for TNFα levels by ELISA. To show the combined influence of all three modifications (sialylation, amide linkage, and phosphorylation) on TNFα levels, the relative abundance of two amide and three amide linkages plus 3 or 4 phosphoryl residues were added to either 100 (for strains containing 2 SA residues) or 50 (for strains containing 1 SA residue). TNFα levels were plotted against this relative score out of 300 for these modifications. Data points represent mean values for an individual strain from a minimum of four independent experiments. Linear regression analyses were performed.

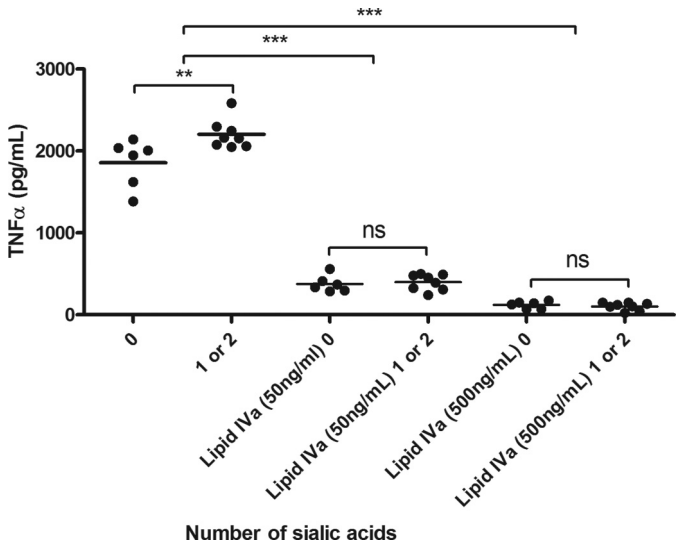

FIGURE 5. ***C. jejuni* LOS modifications modulate TLR4 signaling.** THP-1 cells were stimulated with 10 ng/ml LOS for 20 h in the presence of either a 50 or 500 ng/ml concentration of the TLR4 antagonist lipid IVa, and TNFα levels were assessed by ELISA. Data points represent mean values for an individual strain from a minimum of four independent experiments. One-way analysis of variance was performed (**, $p < 0.01$; *** $p < 0.001$; *ns*, not significant).

also correlated with TNFα levels (Fig. 3*D*; $r = 0.81$; $p = 0.04$). To show the combined influence of all three modifications (sialylation, amide linkage, and phosphorylation) on TNFα levels, the relative abundances of two amide and three amide linkages plus 3 or 4 phosphoryl residues were added to either 100 (for strains containing 2 SA residues) or 50 (for strains containing 1 SA residue). This gave a relative score out of 300 for these modifications. The combination of all three factors showed a strong correlation with TNFα production (Fig. 4*A*; $r = 0.73$; $p = 0.002$). When cells were exposed to 100 ng/ml LOS, the magnitude of cytokine responses increased in parallel, highlighting a clear dose-response effect. In addition, the correlation observed with 10 ng/ml LOS was maintained (Fig. 4*B*; $r = 0.75$; $p = 0.001$). Importantly, infection with live bacteria elicited a correlation strikingly similar to that seen to their corresponding LOS moieties (Fig. 4*C*; $r = 0.81$; $p = 0.0004$). Thirteen of 15 strains showed similar growth rates in culture medium, multiplying ~10-fold in 20 h (data not shown). Two of 15 strains showed limited growth, although this did not alter cytokine induction relative to the purified LOS. The similar pattern of TNFα induction between purified LOS and live infection suggested that the interaction of LOS structural moieties with TLR4 is a major determinant of the immune outcome to *C. jejuni* in human innate immune cells.

The necessity of TLR4 activation was confirmed by utilizing the TLR4 antagonist lipid IVa. The inhibitor caused ablation of TNFα production in a dose-dependent manner (Fig. 5; $p < 0.001$).

The impact of *C. jejuni* LOS modifications was also studied in primary human monocytes (Fig. 6). Sialylation correlated with cytokine induction (Fig. 6*A*; $p < 0.05$ between 0 and 1 SA residue; $p < 0.05$ between 0 and 2 SA residues). Abundance of amide linkages also exerted an effect, although this was not significant (Fig. 6*B*). The presence of 3 or 4 phosphoryl residues correlated with cytokine induction (Fig. 6*C*; $r = 0.7$; $p = 0.02$), and when combined, the modifications showed a significant impact on TNFα levels (Fig. 6*D*; $r = 0.7$; $p = 0.004$). Collectively, the data obtained highlighted the contribution of each LOS structural moiety in modulating and fine-tuning TLR4-mediated responses.

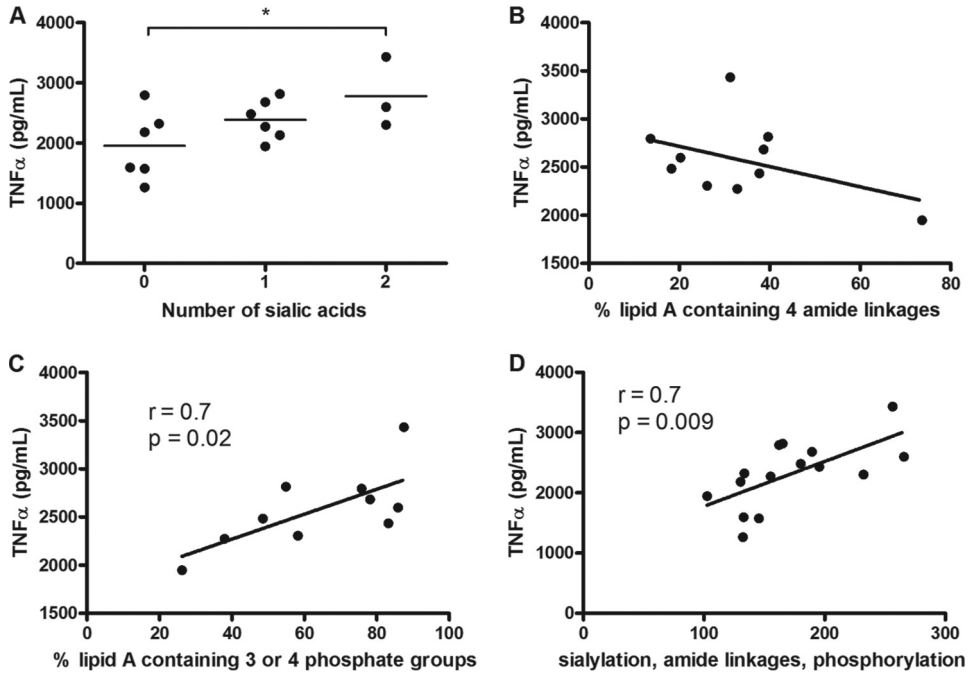

FIGURE 6. **Combinatorial effect of *C. jejuni* LOS sialylation, amide linkages, and phosphorylation on induction of TNFα in primary human monocytes.** Primary monocytes were stimulated with 10 ng/ml LOS for 20 h, and TNFα was assessed by ELISA. TNFα levels were compared with the level of LOS sialylation (*A*), the relative abundance of four amide linkages (*B*), the relative abundance of three or four phosphoryl moieties in each strain (*C*), and a combination of relative sialylation, abundance of amide linkages, and phosphorylation (*D*). Data points represent mean values for an individual strain from five donors. *A*, one-way analysis of variance (*, $p < 0.05$). *B*, *C*, and *D*, linear regression analyses were performed.

DISCUSSION

Analysis of the bacterial LPS/LOS-TLR4 axis is driven by the notion that structural variations can have a major impact on clinical disease outcome; the critical role of *C. jejuni* LOS structure in the onset of GBS is one such example (17). Studies suggest that the SA decoration of *C. jejuni* LOS is an important determinant for the onset of GBS (17) and increased severity of human gastroenteritis (11). In addition, the amide/ester linkages and phosphorylation of the LA can also modulate TLR4 activation (18, 20). However, the relative contribution of natural interstrain variation and the combined effects of these various LOS modifications on human innate immunity require clarification. Herein, we tested the hypothesis that LOS structural modifications not only impact TLR4 function but may also contribute to phylogenetic cluster classification.

LOS moieties from *C. jejuni* human isolates that were associated with the livestock or non-livestock clusters were characterized (21). In combination with genetic analysis, we found structural variations in the OS structures, the number of amide *versus* ester linkages, and the LA phosphorylation status. To gain greater insight into the role of SA in *C. jejuni* recognition, the LOS samples were stratified to represent strains expressing 0, 1, or 2 SA residues. We found a significant correlation between TNFα levels and the degree of sialylation. Importantly, this trend was maintained when tested in human primary monocytes from multiple donors. Abrogation of TNFα in the presence of the TLR4 antagonist lipid IVa indicated that activation of the TLR4 receptor complex was responsible for cytokine production. This is significant as the THP-1 monocytic cell line and primary human monocytes express other receptors (*e.g.* Siglecs) that recognize SA (32). It has also been previously shown that OS sialic acid can directly impact TLR4 signaling in an HEK TLR4 reporter cell line that lacks expression of Siglecs (9). However, no known structural studies have elucidated how sialylation might impact TLR4 recognition and activation; to date, only the inner core OS residues have been shown to interact with the TLR4-MD2 complex, and any potential interactions between the outer core of the OS and the host TLR complex remain ill defined (12). The negative charge of the sialic acid residues, however, may increase affinity for ligand binding, enhancing proinflammatory MyD88-dependent signaling downstream of TLR4. Kuijf *et al.* (9) have previously reported an effect of sialylation on TLR4 function; however, the significance of the degree of sialylation was not explored. By analyzing natural LOS variants, the present study extends our current knowledge of the biological significance of *C. jejuni* LOS sialylation. The SA-dependent increase in TLR4 signaling highlights how this axis may contribute to the increased inflammation and disease severity seen in the presence of *C. jejuni* strains expressing SA-modified LOS (11). However, a similar percentage of SA-expressing strains was associated with diarrhea *versus* asymptomatic carriage, indicating that this moiety plays a minimal role in disease/carriage stratification.

Our report is the first to demonstrate a greater propensity for human *C. jejuni* isolates that genetically associate with livestock strains to contain SA-modified LOS compared with human isolates that genetically associate with non-livestock strains (21). Interestingly, a *C. jejuni* OS truncated mutant strain lacking SA showed reduced colonization in chickens, suggesting that the OS sialylation is a critical determinant for livestock colonization (33). Taken together, the data raise an interesting dichotomy as to the potential role of SA in aiding livestock coloniza-

tion while eliciting a proinflammatory response in humans. The association suggests that the source of *C. jejuni* infection could determine the severity of gastroenteritis and/or the risk levels of developing GBS. SA is known to be involved in immune evasion strategies, a factor that may favor long term colonization of livestock (34). SA decoration can mask bacterial proteins (34), aid in adherence and invasion (35), and mediate evasion of complement-mediated lysis (36). Of note is that *C. jejuni* LOS does not induce a TRIF-dependent IFN-β response in chicken macrophages unlike its human counterpart (5); whether this is responsible for the contrasting chicken *versus* human immune outcomes requires further study.

Variation in *C. jejuni* LA phosphorylation has been reported previously but not quantified (19). We demonstrate that the degree of LA phosphorylation (ranging from ~25–90% LA with three or four phosphate groups) correlates with TNFα expression. No differences between phosphate and PEA groups in the TLR4-stimulatory capacity were observed, similar to our previous analyzes of *N. meningitidis* (24). Studies indicate that PEA modification can also occur on *Campylobacter N*-linked glycoproteins and on the flagellar rod protein, thereby reducing antimicrobial susceptibility (37, 38).

The alteration of *Escherichia coli* LPS from di- to monophosphoryl is known to reduce TLR4 activation (39). The recently elucidated crystal structure of the TLR4-MD2 complex with hexaacylated *E. coli* LPS highlighted the critical importance of LA phosphorylation in the formation of the TLR4-MD2 complex (12). The two phosphate groups form interactions with a cluster of positively charged residues on both MD2 and TLR4, and a hydrogen bond forms with a residue in MD2, aiding the formation of the heterodimer. Mata-Haro *et al.* (40) elegantly showed that monophosphoryl-LA exclusively triggers the TRIF-dependent pathway by activating PI3K, which blocks the MyD88-Mal pathway, in contrast to diphosphorylated LA, which activates the proinflammatory MyD88 pathway. It is interesting to speculate that additional phosphate groups on *C. jejuni* LOS may form additional interactions in the TLR4-MD2 complex, increasing the signaling capacity of the receptor complex and therefore increasing downstream MyD88-dependent cytokine induction. Interestingly, modification of *C. jejuni* LA with both phosphate and PEA residues is more frequent compared with other pathogens that subvert host TLR4. *H. pylori* LpxF actively dephosphorylates its LA, reducing TLR4 activation (41), and commensal *Neisseria* strains lack PEA unlike their pathogenic counterparts (42). *C. jejuni* lacks LpxF,[4] highlighting how these related ϵ-proteobacteria have diverged in LA structure with a potential profound impact on disease outcome. In contrast to sialylation and phosphorylation, alteration of *C. jejuni* LA from ester to amide linkages leads to reduced TLR4 activation (18). In the present study, we quantified the abundance of ester *versus* amide bonds and found a range of ~14–74% LA with four amide linkages. The decreasing proinflammatory response in THP-1 cells and primary monocytes after treatment with *C. jejuni* LA containing fewer ester-linked acyl chains (GlcN-GlcN) suggests that *C. jejuni* may have evolved with modified acyl linkages to dampen TLR4 activation (18). van Mourik *et al.* (18) hypothesize that a reduction in the flexibility of amide linkages compared with ester linkages may influence the formation of the TLR4-MD2 complex. The crystal structure of the TLR4-MD2 complex supports this hypothesis as the LA undergoes a conformation shift upon receptor dimerization that might be impeded if there was reduced flexibility between the acyl chains and the LA backbone (12). Elicitation of similar monocytic cytokine responses between purified LOS and whole bacteria suggested a limited role of intrastrain variation in the present series of experiments. This may reflect a lack of selective pressure under *in vitro* conditions compared with those observed in the *in vivo* setting.

In conclusion, sialylation, phosphorylation, and abundance of ester linkages all combined to affect TLR4 signaling and TNFα expression, suggesting a cumulative impact of these LA modifications on TLR4 activation. Importantly, this phenomenon was similar in response to purified LOS and the corresponding live bacteria, indicating that the *C. jejuni* LOS-TLR4 axis is likely to be a major determinant of early innate immunity to *C. jejuni* in the human host.

Acknowledgments—We gratefully acknowledge the University of California, San Francisco (UCSF) Mass Spectrometry Core Facility, which is supported by the Sandler Family Foundation, the Gordon and Betty Moore Foundation, and National Institutes of Health (NIH)/NCI Cancer Center Support Grant P30 CA082103, and the NIH/National Center for Research Resources (NCRR) Shared Instrumentation Grant S10RR029446-01 (to H. E. Witkowska), and the UCSF Mass Spectrometry Facility (A. L. Burlingame, Director), which is supported by NIH/NCRR Grant P41RR001614.

[4] H. N. Stephenson, C. M. John, N. Naz, O. Gundogdu, N. Dorrell, B. W. Wren, G. A. Jarvis, and M. Bajaj-Elliott, unpublished observations.

REFERENCES

1. Allos, B. M. (2001) *Campylobacter jejuni* infections: update on emerging issues and trends. *Clin. Infect. Dis.* **32,** 1201–1206
2. Gardner, T. J., Fitzgerald, C., Xavier, C., Klein, R., Pruckler, J., Stroika, S., and McLaughlin, J. B. (2011) Outbreak of campylobacteriosis associated with consumption of raw peas. *Clin. Infect. Dis.* **53,** 26–32
3. Kemp, R., Leatherbarrow, A. J., Williams, N. J., Hart, C. A., Clough, H. E., Turner, J., Wright, E. J., and French, N. P. (2005) Prevalence and genetic diversity of *Campylobacter* spp. in environmental water samples from a 100-square-kilometer predominantly dairy farming area. *Appl. Environ. Microbiol.* **71,** 1876–1882
4. Black, R. E., Levine, M. M., Clements, M. L., Hughes, T. P., and Blaser, M. J. (1988) Experimental *Campylobacter jejuni* infection in humans. *J. Infect. Dis.* **157,** 472–479
5. de Zoete, M. R., Keestra, A. M., Roszczenko, P., and van Putten, J. P. (2010) Activation of human and chicken toll-like receptors by *Campylobacter* spp. *Infect. Immun.* **78,** 1229–1238
6. Rathinam, V. A., Appledorn, D. M., Hoag, K. A., Amalfitano, A., and Mansfield, L. S. (2009) *Campylobacter jejuni*-induced activation of dendritic cells involves cooperative signaling through Toll-like receptor 4 (TLR4)-MyD88 and TLR4-TRIF axes. *Infect. Immun.* **77,** 2499–2507
7. Andersen-Nissen, E., Smith, K. D., Strobe, K. L., Barrett, S. L., Cookson, B. T., Logan, S. M., and Aderem, A. (2005) Evasion of Toll-like receptor 5 by flagellated bacteria. *Proc. Natl. Acad. Sci. U.S.A.* **102,** 9247–9252
8. Hu, L., Bray, M. D., Osorio, M., and Kopecko, D. J. (2006) *Campylobacter jejuni* induces maturation and cytokine production in human dendritic cells. *Infect. Immun.* **74,** 2697–2705
9. Kuijf, M. L., Samsom, J. N., van Rijs, W., Bax, M., Huizinga, R., Heikema, A. P., van Doorn, P. A., van Belkum, A., van Kooyk, Y., Burgers, P. C., Luider, T. M., Endtz, H. P., Nieuwenhuis, E. E., and Jacobs, B. C. (2010)

TLR4-mediated sensing of *Campylobacter jejuni* by dendritic cells is determined by sialylation. *J. Immunol.* **185,** 748–755
10. Lepper, P. M., Triantafilou, M., Schumann, C., Schneider, E. M., and Triantafilou, K. (2005) Lipopolysaccharides from *Helicobacter pylori* can act as antagonists for Toll-like receptor 4. *Cell. Microbiol.* **7,** 519–528
11. Mortensen, N. P., Kuijf, M. L., Ang, C. W., Schiellerup, P., Krogfelt, K. A., Jacobs, B. C., van Belkum, A., Endtz, H. P., and Bergman, M. P. (2009) Sialylation of *Campylobacter jejuni* lipo-oligosaccharides is associated with severe gastro-enteritis and reactive arthritis. *Microbes Infect.* **11,** 988–994
12. Park, B. S., Song, D. H., Kim, H. M., Choi, B. S., Lee, H., and Lee, J. O. (2009) The structural basis of lipopolysaccharide recognition by the TLR4-MD-2 complex. *Nature* **458,** 1191–1195
13. Moran, A. P., Zähringer, U., Seydel, U., Scholz, D., Stütz, P., and Rietschel, E. T. (1991) Structural analysis of the lipid A component of *Campylobacter jejuni* CCUG 10936 (serotype O:2) lipopolysaccharide. Description of a lipid A containing a hybrid backbone of 2-amino-2-deoxy-D-glucose and 2,3-diamino-2,3-dideoxy-D-glucose. *Eur. J. Biochem.* **198,** 459–469
14. Moran, A. P., Rietschel, E. T., Kosunen, T. U., and Zähringer, U. (1991) Chemical characterization of *Campylobacter jejuni* lipopolysaccharides containing N-acetylneuraminic acid and 2,3-diamino-2,3-dideoxy-D-glucose. *J. Bacteriol.* **173,** 618–626
15. Parker, C. T., Horn, S. T., Gilbert, M., Miller, W. G., Woodward, D. L., and Mandrell, R. E. (2005) Comparison of *Campylobacter jejuni* lipooligosaccharide biosynthesis loci from a variety of sources. *J. Clin. Microbiol.* **43,** 2771–2781
16. Parker, C. T., Gilbert, M., Yuki, N., Endtz, H. P., and Mandrell, R. E. (2008) Characterization of lipooligosaccharide-biosynthetic loci of *Campylobacter jejuni* reveals new lipooligosaccharide classes: evidence of mosaic organizations. *J. Bacteriol.* **190,** 5681–5689
17. Godschalk, P. C., Heikema, A. P., Gilbert, M., Komagamine, T., Ang, C. W., Glerum, J., Brochu, D., Li, J., Yuki, N., Jacobs, B. C., van Belkum, A., and Endtz, H. P. (2004) The crucial role of *Campylobacter jejuni* genes in anti-ganglioside antibody induction in Guillain-Barré syndrome. *J. Clin. Investig.* **114,** 1659–1665
18. van Mourik, A., Steeghs, L., van Laar, J., Meiring, H. D., Hamstra, H. J., van Putten, J. P., and Wösten, M. M. (2010) Altered linkage of hydroxyacyl chains in lipid A of *Campylobacter jejuni* reduces TLR4 activation and antimicrobial resistance. *J. Biol. Chem.* **285,** 15828–15836
19. Szymanski, C. M., Michael, F. S., Jarrell, H. C., Li, J., Gilbert, M., Larocque, S., Vinogradov, E., and Brisson, J. R. (2003) Detection of conserved *N*-linked glycans and phase-variable lipooligosaccharides and capsules from campylobacter cells by mass spectrometry and high resolution magic angle spinning NMR spectroscopy. *J. Biol. Chem.* **278,** 24509–24520
20. Cullen, T. W., O'Brien, J. P., Hendrixson, D. R., Giles, D. K., Hobb, R. I., Thompson, S. A., Brodbelt, J. S., and Trent, M. S. (2013) EptC of *Campylobacter jejuni* mediates phenotypes involved in host interactions and virulence. *Infect. Immun.* **81,** 430–440
21. Champion, O. L., Gaunt, M. W., Gundogdu, O., Elmi, A., Witney, A. A., Hinds, J., Dorrell, N., and Wren, B. W. (2005) Comparative phylogenomics of the food-borne pathogen *Campylobacter jejuni* reveals genetic markers predictive of infection source. *Proc. Natl. Acad. Sci. U.S.A.* **102,** 16043–16048
22. Hepworth, P. J., Ashelford, K. E., Hinds, J., Gould, K. A., Witney, A. A., Williams, N. J., Leatherbarrow, H., French, N. P., Birtles, R. J., Mendonca, C., Dorrell, N., Wren, B. W., Wigley, P., Hall, N., and Winstanley, C. (2011) Genomic variations define divergence of water/wildlife-associated *Campylobacter jejuni* niche specialists from common clonal complexes. *Environ. Microbiol.* **13,** 1549–1560
23. Gundogdu, O., Mills, D. C., Elmi, A., Martin, M. J., Wren, B. W., and Dorrell, N. (2011) The *Campylobacter jejuni* transcriptional regulator Cj1556 plays a role in the oxidative and aerobic stress response and is important for bacterial survival *in vivo*. *J. Bacteriol.* **193,** 4238–4249
24. John, C. M., Liu, M., and Jarvis, G. A. (2009) Natural phosphoryl and acyl variants of lipid A from *Neisseria meningitidis* strain 89I differentially induce tumor necrosis factor-α in human monocytes. *J. Biol. Chem.* **284,** 21515–21525
25. John, C. M., Liu, M., and Jarvis, G. A. (2009) Profiles of structural heterogeneity in native lipooligosaccharides of *Neisseria* and cytokine induction. *J. Lipid Res.* **50,** 424–438
26. Domon, B. C., and Costello, C. E. (1988) A systematic nomenclature for carbohydrate fragmentations in FAB-MS/MS spectra of glycoconjugates. *Glycoconj. J.* **5,** 397–409
27. Dzieciatkowska, M., Brochu, D., van Belkum, A., Heikema, A. P., Yuki, N., Houliston, R. S., Richards, J. C., Gilbert, M., and Li, J. (2007) Mass spectrometric analysis of intact lipooligosaccharide: direct evidence for O-acetylated sialic acids and discovery of O-linked glycine expressed by *Campylobacter jejuni*. *Biochemistry* **46,** 14704–14714
28. Phillips, N. J., Apicella, M. A., Griffiss, J. M., and Gibson, B. W. (1993) Structural studies of the lipooligosaccharides from *Haemophilus influenzae* type b strain A2. *Biochemistry* **32,** 2003–2012
29. Poltorak, A., He, X., Smirnova, I., Liu, M. Y., Van Huffel, C., Du, X., Birdwell, D., Alejos, E., Silva, M., Galanos, C., Freudenberg, M., Ricciardi-Castagnoli, P., Layton, B., and Beutler, B. (1998) Defective LPS signaling in C3H/HeJ and C57BL/10ScCr mice: mutations in Tlr4 gene. *Science* **282,** 2085–2088
30. Beutler, B. (1990) TNF in pathophysiology: biosynthetic regulation. *J. Invest. Dermatol.* **95,** 81S-84S
31. Liu, M., John, C. M., and Jarvis, G. A. (2010) Phosphoryl moieties of lipid A from *Neisseria meningitidis* and *N. gonorrhoeae* lipooligosaccharides play an important role in activation of both MyD88- and TRIF-dependent TLR4-MD-2 signaling pathways. *J. Immunol.* **185,** 6974–6984
32. Lock, K., Zhang, J., Lu, J., Lee, S. H., and Crocker, P. R. (2004) Expression of CD33-related siglecs on human mononuclear phagocytes, monocyte-derived dendritic cells and plasmacytoid dendritic cells. *Immunobiology* **209,** 199–207
33. Javed, M. A., Cawthraw, S. A., Baig, A., Li, J., McNally, A., Oldfield, N. J., Newell, D. G., and Manning, G. (2012) Cj1136 is required for lipooligosaccharide biosynthesis, hyperinvasion, and chick colonization by *Campylobacter jejuni*. *Infect. Immun.* **80,** 2361–2370
34. Varki, A., and Gagneux, P. (2012) Multifarious roles of sialic acids in immunity. *Ann. N.Y. Acad. Sci.* **1253,** 16–36
35. Louwen, R., Heikema, A., van Belkum, A., Ott, A., Gilbert, M., Ang, W., Endtz, H. P., Bergman, M. P., and Nieuwenhuis, E. E. (2008) The sialylated lipooligosaccharide outer core in *Campylobacter jejuni* is an important determinant for epithelial cell invasion. *Infect. Immun.* **76,** 4431–4438
36. Jarvis, G. A., and Vedros, N. A. (1987) Sialic acid of group B *Neisseria meningitidis* regulates alternative complement pathway activation. *Infect. Immun.* **55,** 174–180
37. Cullen, T. W., Madsen, J. A., Ivanov, P. L., Brodbelt, J. S., and Trent, M. S. (2012) Characterization of unique modification of flagellar rod protein FlgG by *Campylobacter jejuni* lipid A phosphoethanolamine transferase, linking bacterial locomotion and antimicrobial peptide resistance. *J. Biol. Chem.* **287,** 3326–3336
38. Scott, N. E., Nothaft, H., Edwards, A. V., Labbate, M., Djordjevic, S. P., Larsen, M. R., Szymanski, C. M., and Cordwell, S. J. (2012) Modification of the *Campylobacter jejuni N*-linked glycan by EptC protein-mediated addition of phosphoethanolamine. *J. Biol. Chem.* **287,** 29384–29396
39. Cekic, C., Casella, C. R., Eaves, C. A., Matsuzawa, A., Ichijo, H., and Mitchell, T. C. (2009) Selective activation of the p38 MAPK pathway by synthetic monophosphoryl lipid A. *J. Biol. Chem.* **284,** 31982–31991
40. Mata-Haro, V., Cekic, C., Martin, M., Chilton, P. M., Casella, C. R., and Mitchell, T. C. (2007) The vaccine adjuvant monophosphoryl lipid A as a TRIF-biased agonist of TLR4. *Science* **316,** 1628–1632
41. Cullen, T. W., Giles, D. K., Wolf, L. N., Ecobichon, C., Boneca, I. G., and Trent, M. S. (2011) *Helicobacter pylori* versus the host: remodeling of the bacterial outer membrane is required for survival in the gastric mucosa. *PLoS Pathog.* **7,** e1002454
42. John, C. M., Liu, M., Phillips, N. J., Yang, Z., Funk, C. R., Zimmerman, L. I., Griffiss, J. M., Stein, D. C., and Jarvis, G. A. (2012) Lack of lipid A pyrophosphorylation and functional lptA reduces inflammation by *Neisseria* commensals. *Infect. Immun.* **80,** 4014–4026